Atmósfera (1999) 12, pp. 223-243

Simulation of exact barotropic vorticity equation solutions using a spectral model

ISMAEL PEREZ GARCIA and YURI N. SKIBA

Centro de Ciencias de la Atmósfera, UNAM, Circuito Exterior, C. U., 04510, México, D. F., México

(Manuscript received Sept. 1, 1998; accepted in final form April 6, 1999)

RESUMEN

Se usa un modelo espectral numérico de la atmósfera barotrópica con el fin de simular soluciones exactas bien conocidas de la ecuación de vorticidad para un fluido ideal incompresible sobre una esfera en rotación. Se enfatiza en estudiar el comportamiento del error relativo entre la solución exacta y la solución numérica, y en preservar la energía cinética total, la enstrofia integral y la estructura geométrica de las soluciones (flujos zonales, ondas de Rossby-Haurwitz, soluciones de Wu-Verkley, y modones bipolares de Verkley). Las integraciones realizadas con el modelo en un intervalo de 10 días, muestran que las soluciones exactas clásicas se reproducen con buena precisión. Sin embargo, la inestabilidad de unas soluciones exactas generalizadas respecto a los errores iniciales y los errores asociados al forzamiento numérico puede ser un serio obstáculo en simular el comportamiento de dichas soluciones a largo plazo. Si éste es el caso entonces aun el modelo espectral de alto orden de truncación con muy pequeño paso temporal falla en resolver el problema, y las trayectorias de las soluciones numéricas y exactas divergen de una a otra en el tiempo. Por otra parte, la energía total y la enstrofia integral de todas las soluciones calculadas numéricamente se conservan con un alto grado de precisión por lo menos durante los primeros diez días.

ABSTRACT

A numerical spectral model of the barotropic atmosphere is used to simulate well-known exact solutions of the vorticity equation for an ideal incompressible fluid on a rotating sphere. Primary emphasis is received to the behavior of the relative error between the exact and numerical solutions as well as to preserving the total kinetic energy, integral enstrophy, and geometric structure of the solutions (zonal flows, Rossby-Haurwitz waves, Wu-Verkley solutions, and Verkley's dipole modons). The 10-day integrations carried out with the model show that the classical exact solutions (RH waves) can be calculated to a good approximation. However, the instability of some exact generalized solutions with respect to initial errors and the errors associated with nonzero numerical model forcing can be a serious obstacle in simulating long-time behavior of such solutions. If it is the case then even highly truncated model with very small time step fails to resolve the problem, and the paths of the numerical and exact solutions diverge from each other with time. Nevertheless, the total energy and integral enstrophy of all the numerical solutions are conserved with a high degree of precision at least during first 10 days.

1. Introduction

The motion of an ideal non-divergent fluid on the rotating unit sphere S is governed by the barotropic vorticity equation (BVE) which can be written in the non-dimensional form as

$$\Delta\psi_t + J(\psi, \Delta\psi + 2\mu) = 0 \tag{1}$$

where $\psi(t,\ \lambda,\ \mu)$ is the streamfunction, $\varsigma = \Delta\psi$ is the relative vorticity, Δ is the Laplace operator, λ is the longitude, and μ is the sine of latitude. The Jacobian $J(\psi,\ \Delta\psi + 2\mu)$ contains both the nonlinear term $J(\psi,\ \Delta\psi)$ and the sphere rotation term $J(\psi,\ 2\mu) = 2\psi_\lambda$. To the first approximation, the same equation governs unforced and non-dissipative large-scale motions of the barotropic atmosphere (Rossby, 1939; Haurwitz, 1940; Blinova, 1946, 1956; Silberman, 1954; Adem, 1956), and ocean and sea (Gill, 1982; Zalesny, 1986; Bulgakov, 1996).

Physically, exact BVE solutions are helpful, since they provide an explanation for the time-space structure of the waves existing in an ideal incompressible fluid on a rotating sphere. Mathematically, exact BVE solutions can be used in the solution stability study (Hoskins, 1973; McWilliams *et al.*, 1981; McWilliams and Zabusky, 1982; Wu, 1993; Skiba, 1991, 1992a,b; Skiba and Adem, 1998), in testing the numerical BVE models, etc. The simplest example of the exact BVE solution is any zonal flow $\psi(\mu)$. Haurwitz (1940) was the first who generalized Rossby's (1939) wave solutions to the spherical geometry by using the spherical harmonics $Y_n^m(\lambda,\ \mu)$. In what follows, Ertel (1943), Craig (1945), Blinova (1946, 1956), Neamtan (1946) and Rochas (1986) suggested various modifications of the Rossby-Haurwitz (RH) solutions, while Thompson (1982) gave the most general form of a global and smooth BVE solution

$$\psi(t,\ \lambda,\ \mu) = Y(\lambda',\ \mu') - \omega\mu + \ Const \tag{2}$$

that is the sum of a spherical harmonic $Y(\lambda',\ \mu')$, a term representing the sphere rigid rotation with angular velocity ω, and a constant. The primed coordinates $(\lambda',\ \mu')$ are related here with a new geographical system of coordinates whose pole moves along a specific latitudinal circle of the fixed system $(\lambda,\ \mu)$ with a constant velocity

$$c = [2 + \omega(2 + \chi)]/\chi \tag{3}$$

where χ is the eigenvalue of the spectral problem $\Delta Y = \chi Y$ for Laplace operator on the unit sphere. In particular,

$$\chi = \chi_n = -n(n+1) \tag{4}$$

for the spherical harmonic $Y(\lambda',\ \mu')$ of integer degree n.

In the theory of differential equations, the waves (2) are called classical solutions as differentiated from the generalized solutions which are not so smooth being the weak limits of the convergent sequences of smooth functions. Szeptycki (1973) was the first to prove the existence and uniqueness of a generalized BVE solution on a sphere. The first generalized isolated solutions of equation (1) named dipole and monopole modons were originally constructed by Tribbia (1984) and Verkley (1984, 1987, 1989, 1990) by using two spherical harmonics of different degrees. These modons are spherical analogues of the isolated vortex solutions constructed on the plane by Stern (1975), Larichev and Reznik (1976), and Berestov (1979) (see also Kanehisa, 1994). Later on, Neven (1992, 1993) has given generalized isolated solutions in the form of a quadrupole

modon, while Wu and Verkley (1993) suggested generalized global solutions composed of two RH waves. Characteristic of the generalized solutions is their low smoothness on a sphere: in the general case, the derivatives of the third order of the solution streamfunction are not continuous on the whole sphere. However, it is easy to show that a stationary dipole modon by Verkley (1984) is the classical BVE solution. Indeed,

$$J(\psi,\ \Delta\psi) = -r(\lambda',\ \mu')\frac{\partial\psi}{\partial\lambda}$$

where

$$r(\lambda',\ \mu') = \begin{cases} c\chi_\alpha + 2, & \text{if } (\lambda',\ \mu')\epsilon S_i \\ c\chi_\sigma + 2, & \text{if } (\lambda',\ \mu')\epsilon S_o. \end{cases}$$

Thus if $c = 0$ then the Jacobian term in (1) is continuous everywhere on the sphere (Skiba, 1993). While the RH and Wu-Verkley waves have turned out to be useful in understanding global wave structures in the atmosphere, the modons have been beneficial in interpreting some localized stable atmospheric structures associated with blocking events (Stern, 1975; McWilliams *et al.*, 1981; McWilliams and Zabusky, 1982; Verkley, 1989).

In the present work, zonal flows, RH waves, Wu-Verkley solutions and dipole modons by Verkley (1984) are simulated with a numerical spectral barotropic atmosphere model of the Center for Atmospheric Sciences (UNAM, Mexico). The work is considered as preliminary to the numerical study of the asymptotic behavior and stability of solutions to a forced and dissipative barotropic atmosphere model (Wiin-Nielsen, 1979; Andrews, 1984; Temam, 1988; Skiba, 1994, 1996, 1997) and low-frequency variability in the atmosphere (Branstator, 1985; Legras and Ghil, 1985; Wu, 1993). The accuracy of reproducing the analytical solutions with the numerical spectral model was controlled by means of four parameters: the total energy and integral enstrophy of the numerical solutions, and the absolute and relative errors estimated with $L_2(S)$-norm. The 10-day integration results obtained show that the classical solutions (RH waves) can be calculated to a good approximation. However, the instability of some exact generalized solutions with respect to initial errors and the errors associated with nonzero numerical (artificial) model forcing can be a serious obstacle in simulating long-time behavior of such solutions. If it is the case then even highly truncated model with very small time step fails to resolve the problem, and the paths of the numerical and exact solutions diverge from each other with time. Nevertheless, the total energy and integral enstrophy of all the numerical solutions are conserved with a high degree of precision at least during first 10 days.

2. Invariants of motion and approximation errors

It is well known that the behavior of a BVE solution is subjected to infinite number of restrictions (Dikii, 1976). In particular, the total kinetic energy

$$K = \frac{1}{2}\int_S |\ \nabla\psi\ |^2\, dS, \tag{5}$$

the enstrophy

$$E = \frac{1}{2}\int_s |\varsigma|^2 \, dS = \frac{1}{2}\int_s |\Delta\psi|^2 \, dS, \tag{6}$$

and hence, the average spectral number E/K of each BVE solution are conserved with time (Fjörtoft, 1953). Moreover, any smooth function $f(\Delta\psi + 2\mu)$ of the absolute vorticity $\Delta\psi + 2\mu$ is also invariant of motion (Casimir function). For instance, for a natural k, the value

$$\| \Delta\psi + 2\mu \|_{L_{2k}} = \left(\int_S |\Delta\psi + 2\mu|^{2k} \, dS \right)^{1/2k} \tag{7}$$

is constant with time and represents the L_{2k}-norm of the absolute vorticity. Note that the more is k, the stronger is the norm. In the particular case that $k = 1$, this norm is equivalent to the enstrophy norm $\sqrt{E}$ or the 2-norm (14) defined below. Piterbarg (1998) has recently shown that there exist no independent invariants for equation (1) except for the energy, enstrophy, meridional momentum and Casimir functions.

The spectral model of the vorticity equation (1) was introduced and analyzed in many works (Silberman, 1954; Merilees, 1968). The model is based on using Fourier-Laplace series (Topuriya, 1987). A discrete spectral model is obtained by truncating Fourier-Laplace series for the stream-function, vorticity and Jacobian (Baer and Platzman, 1961; Platzman, 1960, 1962; Baer, 1964; Ellsaesser, 1966; Machenhauer, 1979). We have used the triangular truncation

$$f_N \equiv T_N f = \sum_{n=1}^{N} \sum_{m=-n}^{n} f_n^m Y_n^m \tag{8}$$

of each function

$$f = \sum_{n=1}^{\infty} \sum_{m=-n}^{n} f_n^m Y_n^m. \tag{9}$$

Thus f_N represents the orthogonal projection of f on a finite dimensional subspace of the spherical polynomials of the degree N (Richtmyer, 1981). This subspace is the orthogonal sum of subspaces H_n of the homogeneous spherical polynomials of the degree n (Helgason, 1984). We suppose that the spherical harmonics Y_n^m are normalized by

$$< Y_n^m, \; Y_k^l >= \delta_{nk}\delta_{ml}$$

where

$$< \phi, \; \psi >= \int_S \phi\bar{\psi} dS$$

is the inner product of two functions on the unit sphere.

The truncation (8) introduces a spatial approximation error whose magnitude depends on the truncation number N and smoothness of the function f. Since the spectral method consumes a lot of computer time, it is always desirable to decrease the truncation number. However, in a truncated spectral model, there is an artificial accumulation of the kinetic energy in the small scales, due to nonlinear interactions (Mesinger and Arakava, 1976). This process breaks the balanced energy cascades to the large and small scales peculiar to equation (1) (Fjörtoft, 1953; Longuet-Higgins and Gill, 1967; Merilees and Warn, 1975; Boer, 1983). The problem is aggravated as the truncation number decreases. Moreover, the discretization of the differential barotropic atmosphere model in time introduces additional time approximation error that breaks almost all of the infinite number of the invariants of motion characteristic of an ideal incompressible fluid on a rotating sphere. In particular, the leap-frog scheme used here preserves the global mean kinetic energy (5) and enstrophy (6) just approximately. The evolution of these characteristics of the BVE solutions provides a useful check on the spectral BVE model and was of decisive importance in choosing the leap-frog scheme between several explicit schemes subjected to this test, including the second-, third- and fourth-order Adams-Bashforth methods (Golub and Ortega, 1992). Moreover, all the exact BVE solutions known up to now conserve its geometric form in a rotating system of coordinates (equation (1) possesses a group of zonal translations). Thus, the conservation of the geometric structure of solutions also characterizes the quality of the spectral BVE model. However, the absolute and relative errors of the calculation of exact solutions to the barotropic vorticity equation are the best indicators of the spectral model quality.

In the course of integrating the spectral model truncated by a number N, we will monitor the behavior of the global mean kinetic energy $\overline{\mathrm{K}} = K_N/4\pi$ and global mean enstrophy $\overline{\mathrm{E}} = E_N/4\pi$ of the numerical solution where

$$K_N = -\frac{1}{2}\sum_{n=1}^{N}\chi_n \sum_{m=-n}^{n} \mid \psi_n^m \mid^2 = \sum_{n=1}^{N} K_n, \tag{10}$$

$$E_N = \frac{1}{2}\sum_{n=1}^{N}\sum_{m=-n}^{n} \mid \varsigma_n^m \mid^2 = -\sum_{n=1}^{N} \chi_n K_n, \tag{11}$$

$\psi_n^m = <\psi,\ Y_n^m>$, $\varsigma_n^m = <\varsigma,\ Y_n^m> = <\Delta\psi,\ Y_n^m>$, χ_n is defined by (4), and

$$K_n = -\frac{1}{2}\chi_n \sum_{m=-n}^{n} \mid \psi_n^m \mid^2 \tag{12}$$

is the part of the total energy concentrated in the orthogonal subspace H_n of the homogeneous spherical polynomials of the degree n. Evidently, as truncation number N tends to infinity, the energy sum (10) converges faster than the enstrophy sum (11). Generally, the rate of convergence of the Fourier-Laplace series of a function $f(\lambda,\ \mu)$ on the sphere is estimated as

$$\| f - f_N \|_s \equiv \| (I - T_N) f \|_s \leq N^{-r} \| f \|_{s+r} \tag{13}$$

where I is the identity operator, s is real, r is real and positive, and

$$|| f ||_s = \left\{ \sum_{n=1}^{\infty} \chi_n^s \sum_{m=-n}^{n} | f_n^m |^2 \right\}^{1/2} \tag{14}$$

is the s-norm of the function (Skiba, 1989, 1994, 1998). Note that if the norm $|| f ||_{s+r}$ of a function f is finite then $|| f ||_s$ is also finite due to the inequality

$$|| f ||_s \leq 2^{-r/2} || f ||_{s+r} \tag{15}$$

(Skiba, 1989). Thus the smoothness of a function f on a sphere can be characterized by the highest number s such that norm (14) is finite, that is, the serie in (14) converges. Then, by (13), the smoother is the function, the faster is the convergence of its Fourier series.

We now estimate the error δJ introduced by truncating the Jacobian term in (1). This error can be considered as artificial forcing in the numerical model. Let ψ be an exact solution of the BVE, and $|| T_N ||$ be the operator norm induced by the 0-norm (14). Due to (8) and (9), $|| T_N || \leq 1$ Then taking into account the orthogonal decomposition $f = T_N f + (I - T_N) f$ we have

$$\delta J \equiv || J(\psi,\ \Delta\psi) - T_N J(\psi_N,\ \Delta\psi_N) ||$$

$$\leq || T_N \{ J(\psi,\ \Delta\psi) - J(\psi_N,\ \Delta\psi_N) \} || + || (I - T_N) J(\psi,\ \Delta\psi) ||$$

$$\leq || J(\psi - \psi_N,\ \Delta\psi) || + || J(\psi_N,\ \Delta(\psi - \psi_N)) || + || (I - T_N) J(\psi,\ \Delta\psi) || \tag{16}$$

where $|| \psi ||$ is the 0-norm (14): $|| \psi ||_o = < \psi,\ \psi >^{1/2}$. Using the estimate

$$|| J(\psi,\ \phi) || \leq C\, ||_\psi ||_{1/2} || \phi ||_{1/2} \tag{17}$$

(see formulas (16), (26) and (51) in Skiba, 1998), and inequalities (13) and (15) one can obtain

$$\delta J \leq C(|| \psi - \psi_N ||_{1/2} || \Delta\psi ||_{1/2} + || \psi_N ||_{1/2} || \Delta(\psi - \psi_N) ||_{1/2}) + N^{-r} || J(\psi,\ \Delta\Psi) ||_r$$

$$\leq N^{-r} \{ C(|| \psi ||_{r+1/2} || \Delta\psi ||_{1/2} + || \psi ||_{1/2} || \Delta\psi ||_{r+1/2}) + || J(\psi,\ \Delta\psi) ||_r \}$$

$$\leq N^{-r} (R || \Delta\psi ||^2_{r+1/2} + || J(\psi,\ \Delta\psi ||_r). \tag{18}$$

where $r > 0$, and C and R are some constants independent of ψ. By (18), the approximation error decreases as both the truncation number N and the smoothness r of functions $\Delta\psi$ and $J(\psi,\ \Delta\psi)$ grow. Thus we expect that numerical error δJ will be least for a smooth RH-wave solution ψ, and most for a modon solution. Moreover, such error is larger for a large-amplitude modon rather than for a small-amplitude modon. These conclusions coincide with those previously made by McWilliams and Zabusky (1982) and Blender (1992) for modon solutions on the plane.

3. Simulation of analytical solutions

It should be noted that though the equation (1) and its analytical solutions are given in this paper in the non-dimensional form, all the numerical experiments have been carried out with a dimensional version of the model. The results presented in this section can be transformed to the non-dimensional form using the well-known relations

$$t = \Omega^{-1} t^*, \quad \psi = \Omega a^2 \psi^*, \quad \Delta = a^{-2} \Delta^*, \quad J = a^{-2} J^* \tag{19}$$

between the dimensional and non-dimensional (asterisked) values of the time, streamfunction, Laplace operator, and Jacobian, respectively. Here $\Omega = \pi/43200$ is the angular velocity of the Earth rotation, and a is the Earth radius. The corresponding relationships for the total energy (5) and enstrophy (6) are

$$K = a^4 \Omega^2 K^*, \quad E = a^2 \Omega^2 E^*.$$

Also, instead of the non-dimensional formula $\psi_n^{*m} = \chi_n^{-1} \zeta_n^{*m}$ where χ_n is defined by (4), Fourier's coefficients of the dimensional streamfunction ψ and relative vorticity $\zeta = \Delta\psi$ are related to each other by

$$\psi_n^m = a^2 \chi_n^{-1} \zeta_n^m. \tag{20}$$

We now describe some results of testing the numerical spectral barotropic atmosphere model by using a few different types of analytical BVE solutions.

1) *Zonal flow.* First, we have approximated zonal BVE solution $\psi(\mu)$ by

$$\psi_N(\mu) = \sum_{n=0}^{N} \psi_n P_n(\mu) \tag{21}$$

where $P_n(\mu)$ is the Legendre polynomial of degree n. The streamfunctions of the corresponding numerical solutions have been calculated for 240 hours. In all the experiments carried out with various numbers N, the Jacobian term of the numerical scheme was equal to zero, and there were no oscillations of the global mean energy and enstrophy. The geometric structure of the numerical zonal solutions is conserved with time (not shown here), and the accuracy of reproducing the analytical solution depends only on the truncation number N. Besides initial truncation error (zonal perturbation) does not grow with time (Skiba and Adem, 1998).

2) *Rossby-Haurwitz wave.* For each n, we can find a numerical BVE solution initially equal to

$$\psi(\lambda,\ \mu,\ 0) = -\omega\mu + \sum_{m=-n}^{n} \psi_n^m Y_n^m(\lambda,\ \mu) \tag{22}$$

and compare it with the corresponding analytical solution

$$\psi(\lambda,\ \mu,\ t) = -\omega\mu + \sum_{m=-n}^{n} \psi_n^m Y_n^m(\lambda - c_n t,\ \mu)$$

where c_n and χ_n are defined by (3) and (4), respectively. The solution is a zonally propagating RH wave of the subspace $H_1 \oplus H_n$. In particular, the streamfunction of the numerical RH-wave

$$\psi(\lambda,\ \mu,\ t) = -\omega\mu + \psi_n^m P_n^m(\mu) \cos m(\lambda - c_n t) \tag{23}$$

where $n = 3$, $m = 1$ and $\psi_n^m = \omega = 337.59 \cdot 10^{-5}$ is given in Figure 1 at $t = 0$ (a) and after 240 hours of integrating the spectral T31-model (b). Hereafter, all the streamfunction fields presented have been premultiplied by 10^{-7}. One can see that the numerical solution moves to the west without changing its geometric structure and is in close agreement with the analytical solution (23). The wave makes one rotation around the Earth per about 6 days. The global mean energy and enstrophy of the solution show very small variations not exceeding $7 \cdot 10^{-4}\%$ and $4.10^{-4}\%$, respectively (Fig.1c-d). These oscillations are due to using the leap-frog scheme without filtering the numerical mode (Gary, 1979; Morton and Mayers, 1994). The 10-day integrations carried out with various RH waves (different n) show that these solutions are well reproduced. Besides, the larger is the spatial scale of the wave, the better is the accuracy. It can be explained by the following reasons. First, there is no initial error associated with the solution

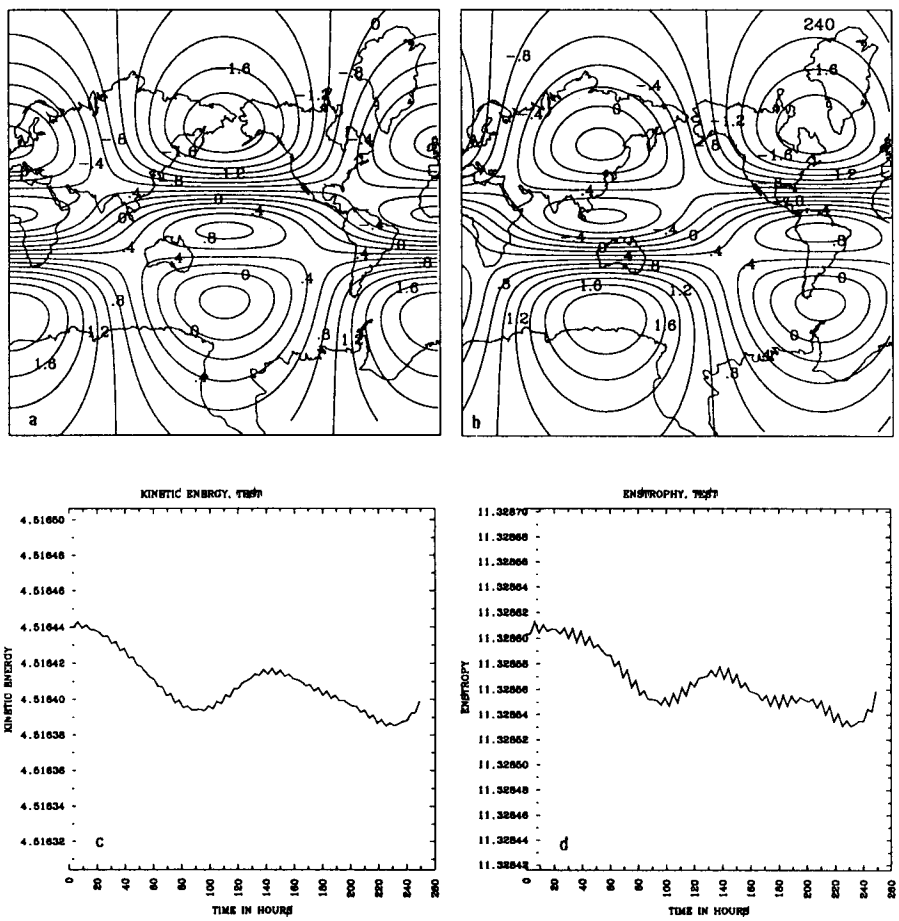

Fig.1. The streamfunction of numerical RH solution (23) at initial moment (a), and after 240 hours of integrating the T31-model (b). Evolution of the global mean kinetic energy (c) and enstrophy (d) of solution (23).

truncation (always $N \geq n$). Second, artificial numerical forcing introduced in the model by the errors of calculating the Jacobian is almost zero. In addition, due to estimate (18), truncation errors decrease rapidly as the truncation number N increases, since the RH wave is an infinitely smooth solution. And finally, the RH wave appears to be rather stable to small-scale model errors associated with the artificial forcing. In order to test the quality of numerical results we used the absolute and relative errors defined by

$$AE = \| \psi_N - \psi \| \qquad RE = \frac{\| \psi_N - \psi \|}{\| \psi \|} \tag{24}$$

where ψ_N and ψ are the numerical and analytical streamfunction solutions, respectively. The behavior of the relative errors for different solutions is given in Figure 6. It is seen that the relative error for the RH wave slowly grows with time mainly due to a lag of the numerical wave (Fig. 6, curve A).

3) *Wu-Verkley solution.* Also, we have reproduced numerically a Wu-Verkley (1993) solution whose streamfunction has the form

$$\psi(\lambda,\ \mu,\ t) = Y_i(\lambda - ct, \mu) - \omega_i \mu + D_i \tag{25}$$

in ith sphere region $R_i (i = 1, 0, 2)$ where

$$R_1 = \{(\lambda,\ \mu) : \mu \epsilon [\mu_o,\ 1]\}, \quad R_o = \{(\lambda,\ \mu) : \mu \epsilon [-\mu_o,\ \mu_o]\}, \quad R_2 = \{(\lambda,\ \mu) : \mu \epsilon [-1,\ -\mu_o]\},$$

$0 < \mu_o < 1$, ω_i and D_i are constant, Y_i is an eigenfunction of the spectral problem

$$\Delta Y_i = \chi_i Y_i \tag{26}$$

for the Laplace operator, and

$$c = [2 + \omega_i (2 + \chi_i)]/\chi_i. \tag{27}$$

Following to Wu and Verkley (1993), we have taken

$$Y_1(\lambda - ct,\ \mu) = A_1 P_\alpha^o(\mu) + B_1 P_\alpha^m(\mu) \cos m(\lambda - ct)$$

$$Y_o(\lambda - ct,\ \mu) = A_o T_\sigma^o(\mu) + B_o T_\sigma^m(\mu) \cos m(\lambda - ct)$$

$$Y_2(\lambda - ct,\ \mu) = -A_1 P_\alpha^o(-\mu) + B_1 P_\alpha^m(-\mu) \cos m(\lambda - ct)$$

where $P_\sigma^m(\mu)$ is the associated Legendre function, and

$$T_\sigma^m(\mu) = P_\sigma^m(\mu) - P_\sigma^m(-\mu), \qquad (m = 0,\ 1,\ 2,\ 3, \ldots). \tag{28}$$

To render the whole solution antisymmetric we have chosen $\omega_2 = \omega_1$, $D_2 = -D_1$ and $\chi_2 = \chi_1$ where

$$\chi_1 = -\alpha(\alpha + 1), \quad \chi_o = -\sigma(\sigma + 1). \tag{29}$$

Thus the total solution (25) consists of a zonal part depending only on μ and a wave part depending on both μ and λ. Due to the continuity conditions (21), (22) by Wu and Verkley (1993), both the zonal and wave parts of the streamfunction, velocity and vorticity of the Wu-Verkley solution (25) are continuous on the whole sphere. The angular phase speed (27) of the solution is arbitrary, since $\omega_2 = \omega_1$ is arbitrary, and a unique set of values for A_1, A_o and $D_o - D_1$ is obtained for a given $\omega_2 = \omega_1$. Note that although the ratio B_o/B_1 is determined by the continuity condition, the wave amplitude of the solution is arbitrary. A solution (25) exists only under two nonlinear constraints on m, μ_o, α and σ:

$$P_\alpha^m(\mu_o) = T_\sigma^m(\mu_o) = 0 \tag{30}$$

For $m = 2$, $\mu_o = \sin 29.998$, $\alpha = 4.542$, and $\sigma = 5.7704672$, the streamfunction of the stationary Wu-Verkley solution calculated numerically is presented in Figure 2 at initial moment (a), and after 48 hours (b), 96 hours (c) and 240 hours (d) of integrating the spectral T31-model.

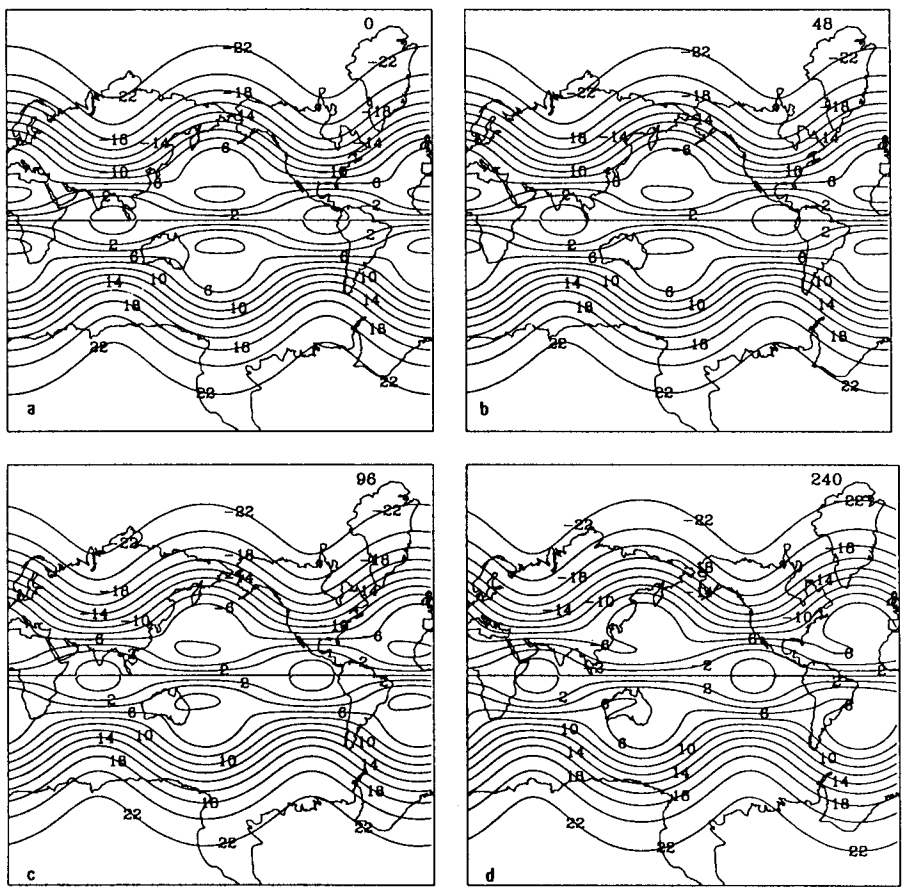

Fig. 2. The streamfunction of numerical Wu-Verkley's solution (25) at initial moment (a), and after 48 hours (b), 96 hours (c) and 240 hours (d) of integrating the T31-model.

The numerical solution conserves well its geometric form during 10 days and is in reasonably good agreement with the analytical Wu-Verkley solution (25). However, unlike the exact stationary modon, the numerical solution moves very slowly to the west. The growth rate of the relative error (24) for the Wu-Verkley solution is rather slow (Fig. 6, curve B), but higher than in the case of the RH wave (Fig. 6, curve A). Moderate absolute and relative errors obtained in calculating this solution show that it appears to be quite stable to small-size initial and model errors. It is in good agreement with the results by Wu (1993) showing that the fastest growing normal modes of the solution (25) possess very large scales rather than small scales. The evolution of the global mean kinetic energy and enstrophy of the Wu-Verkley solution is shown in Fig. 3. It is seen that variations in both the kinetic energy and the enstrophy do not exceed 5.10^{-5}%.

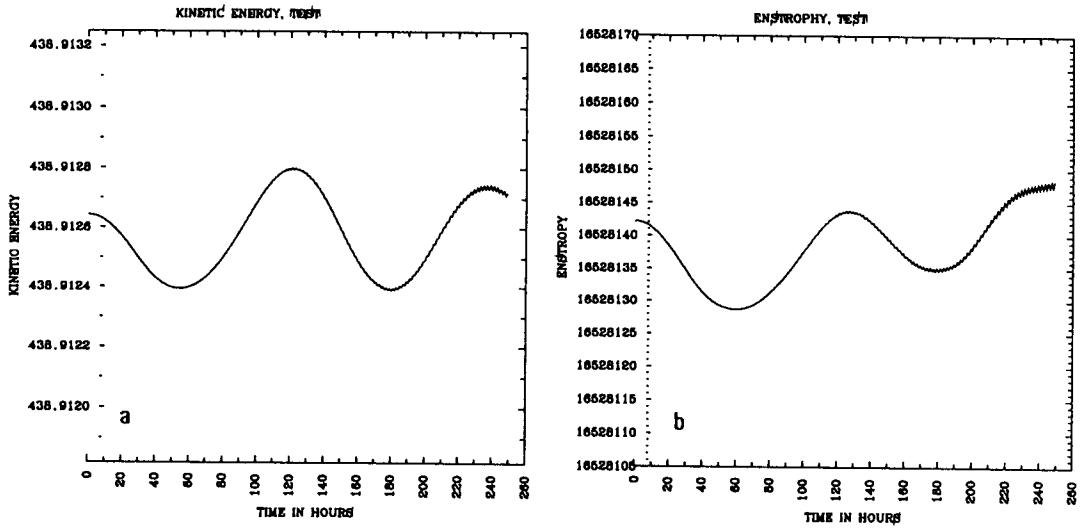

Fig. 3. Evolution of the global mean kinetic energy and enstrophy (premultiplied by 10^{17}) of the numerical Wu-Verkley's solution given in Figure 2.

4) *Dipole modon by Verkley (1984).* This solution of vorticity equation (1) can be written as

$$\psi(\lambda,\ \mu,\ t) = X(\lambda',\ \mu') - \omega\mu + D \tag{31}$$

Here ω is the angular velocity of solid-body rotation in outer region of the modon, D is a constant, and function

$$X(\lambda',\ \mu') = X^d(\mu') \cdot \cos\lambda' + X^m(\mu') \tag{32}$$

consists of a dipole and monopole components, besides,

$$X^d(\mu') = (c-\omega)\sqrt{1-\mu_a^2}\sqrt{1-\mu_o^2} f^d(\mu'), \tag{33}$$

$$X^m(\mu') = (c-\omega)\mu_o\sqrt{1-\mu_a^2} f^m(\mu'), \tag{34}$$

where $\mu_o = \sin\phi^o$, $\mu_a = \sin\phi_a$, ϕ^o is the $(\lambda,\ \mu)$-latitude of the modon center, ϕ_a is the $(\lambda',\ \mu')$-

latitude separating the inner and outer parts of the modon, c is the modon velocity, ω is the angular velocity. The parts $f^d(\mu')$ and $f^m(\mu')$ are defined as

$$f^d(\mu) = \begin{cases} -bB(1,1,\mu) + (1+b)\left(\frac{1-\mu^2}{1-\mu_a^2}\right)^{1/2}, & \text{if } \mu \geq \mu_a, \\ P(1,1,-\mu), & \text{if } \mu < \mu_a. \end{cases} \tag{35}$$

and

$$f^m(\mu) = \begin{cases} -bB(0,1,\mu) + (1+b)\frac{\mu-\mu_a}{\sqrt{1-\mu_a^2}} - P(0,1,-\mu_a) + bB(0,1,\mu_a), & \text{if } \mu \geq \mu_a, \\ -P(1,1,-\mu), & \text{if } \mu < \mu_a. \end{cases} \tag{36}$$

where

$$B(r,\ s,\ \mu) = \frac{P_\alpha^r(\mu)}{P_\alpha^s(\mu_a)}, \qquad P(r,\ s,\ \mu) = \frac{P^r_{-0.5+ik}(\mu)}{P^s_{-0.5+ik}(-\mu_a)} \tag{37}$$

$b = \frac{(k^2+\frac{1}{4})+2}{\alpha(\alpha+1)-2}$, and $P_\gamma^\varepsilon(\mu)$ is the associated Legendre function. The equation

$$B(1,2,\mu_a) = b \cdot P(1,2,-\mu_a) \tag{38}$$

is the necessary condition for the modon to exist.

First we calculated a slowly moving (quasi-stationary) small-size dipole modon defined by $k = 10$, $\alpha = 10$, $\mu_a = \sin 66.14^o$, and $D_o = 0$. The model time step was $\Delta t = 60'$. The streamfunction of the numerical solution is given at the initial moment when the modon center is in the point $\mu_o = 0$, $\lambda_o = 270^o$ (Fig.4a), and after 240 hours of integrating the T31-model (Fig. 4b). There is no significant difference between the small-size modons calculated by using truncations T20 and T31. Thus at least during 10 day-integration, the numerical modon is in a reasonably good agreement with analytical Verkley's solution (31) and conserves its local geometric structure rather well. However, as follows from Figure 6, the small modon is more unstable than the RH wave and Wu-Verkley solution, since the growth rate of its relative error (24) is higher (Fig. 6, curve C). The similar behavior demonstrate small-scale modons on the beta-plane. In order to test the model, we have simulated the behavior of a large-scale Verkley's modon ($k = 2$, $\alpha = 3$, $\mu_o = 0$, $\lambda_o = 270^o$, $\mu_a = \sin 16^o$, and $D_o = 0$) that moves too fast (one revolution per about 19 hours). Unlike the small modon, this rapidly moving modon holds its form well only during 8-days if the model time step is very small: $\Delta t = 20''$ (Fig. 4c-d). During this period the variations in the kinetic energy and enstrophy do not exceed $2.10^{-3}\%$ for the small-size modon (Fig. 5a-b), and $10^{-5}\%$ for the large-size one (Fig. 5c-d). After 8 days, variations in the kinetic energy and enstrophy become larger, there appear small-scale distortions, and the growth rate of the modon relative error increase. The experiments show that in order to improve the accuracy of the calculations by decreasing Courant number, it is necessary to decrease time step and filter the numerical mode of the leap-frog scheme. The following experiment on the interaction of modons confirms the opinion that the modon is quite stable to small-scale perturbations (McWilliams *et al.*, 1981; McWilliams and Zabusky, 1982).

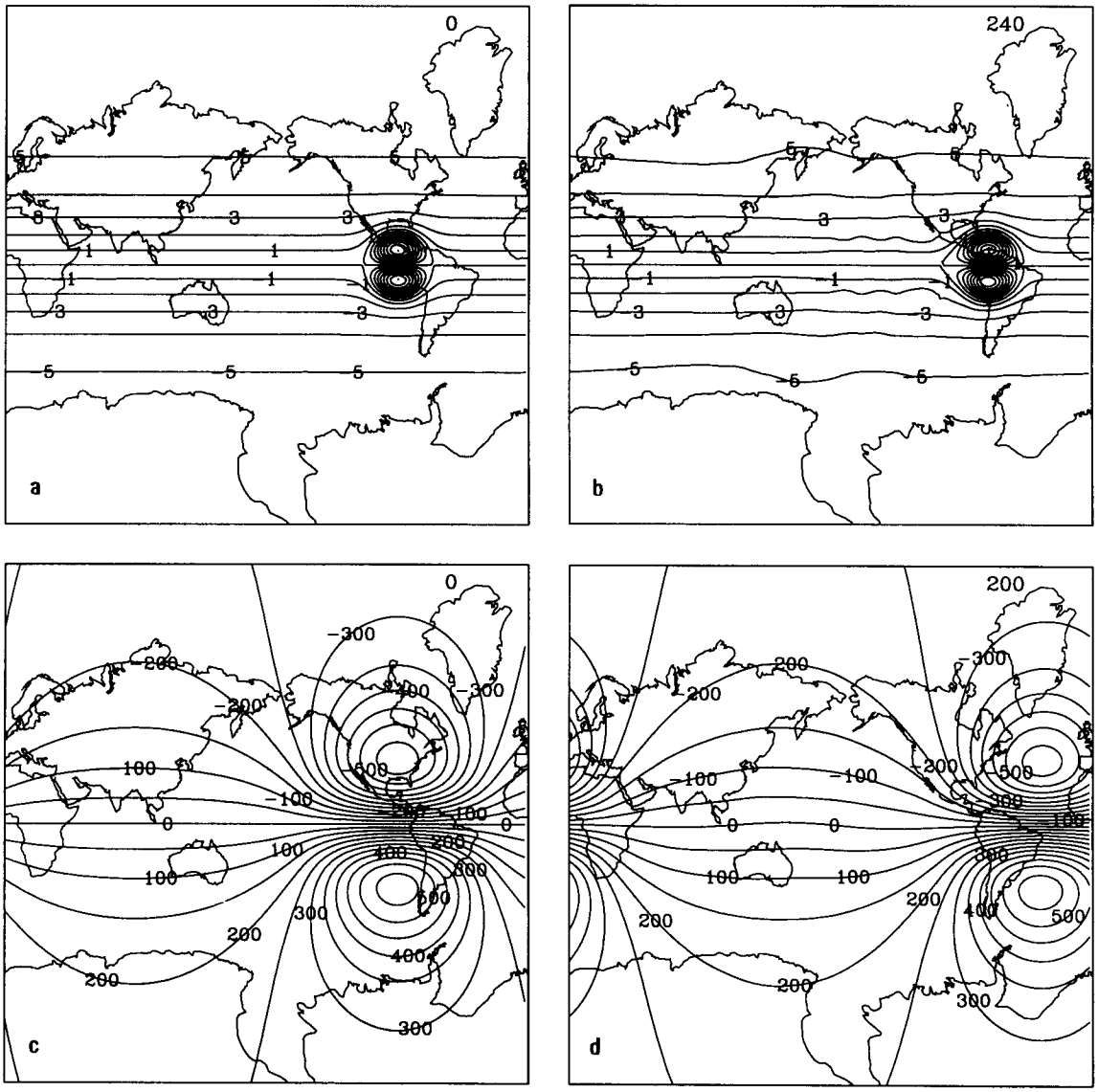

Fig. 4. The streamfunction of a quasi-stationary small-size modon at initial moment (a) and after 240 hours (b), and fast moving large-size modon at initial moment (c) and after 200 hours (d). The contour interval is 1 m^2/s (small-size modon) and 50 m^2/s (large-size modon).

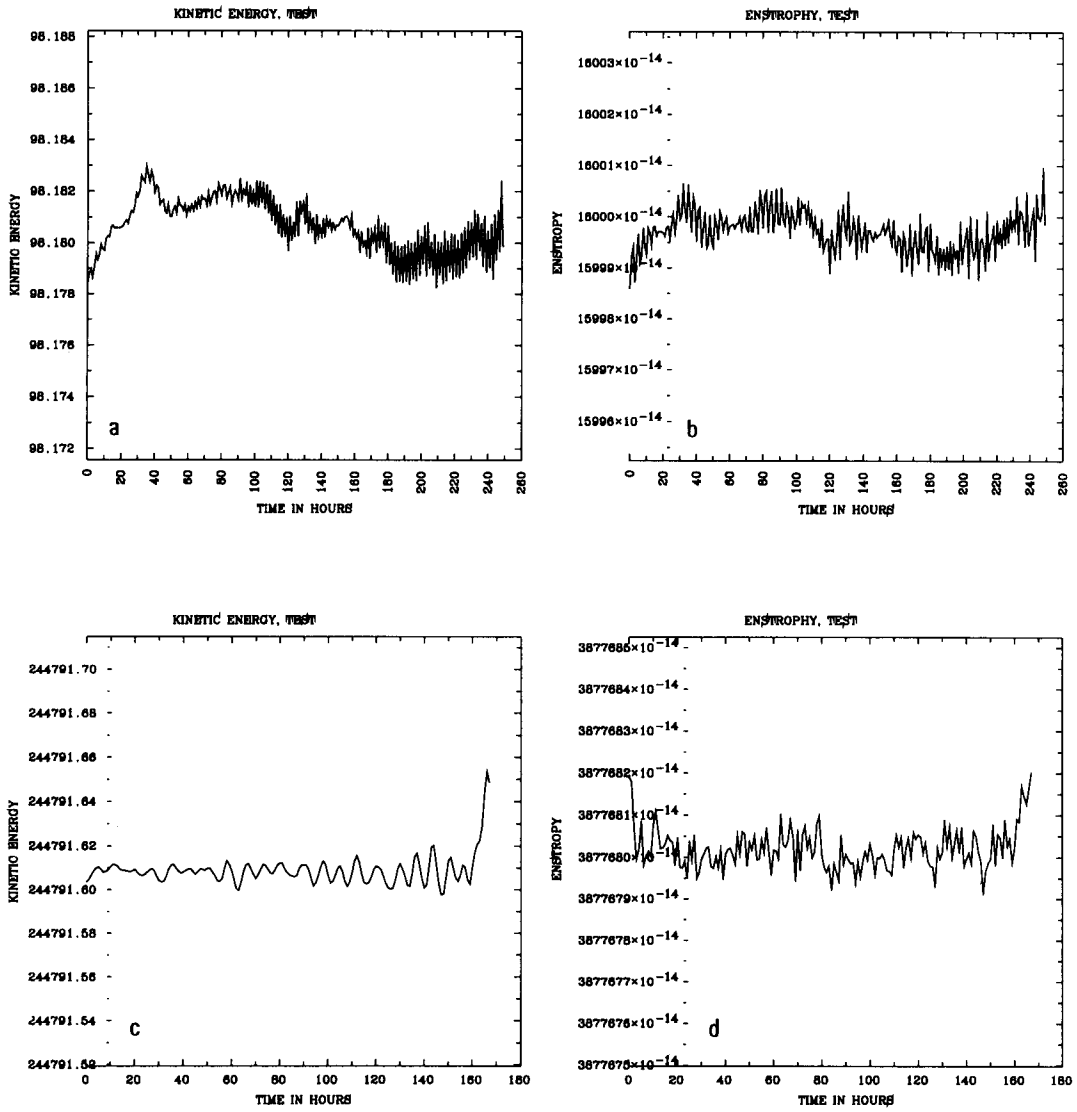

Fig. 5. Evolution of the global mean kinetic energy and enstrophy of the small-size modon (a)-(b) and large-size modon (c)-(d) presented in Fig.4.

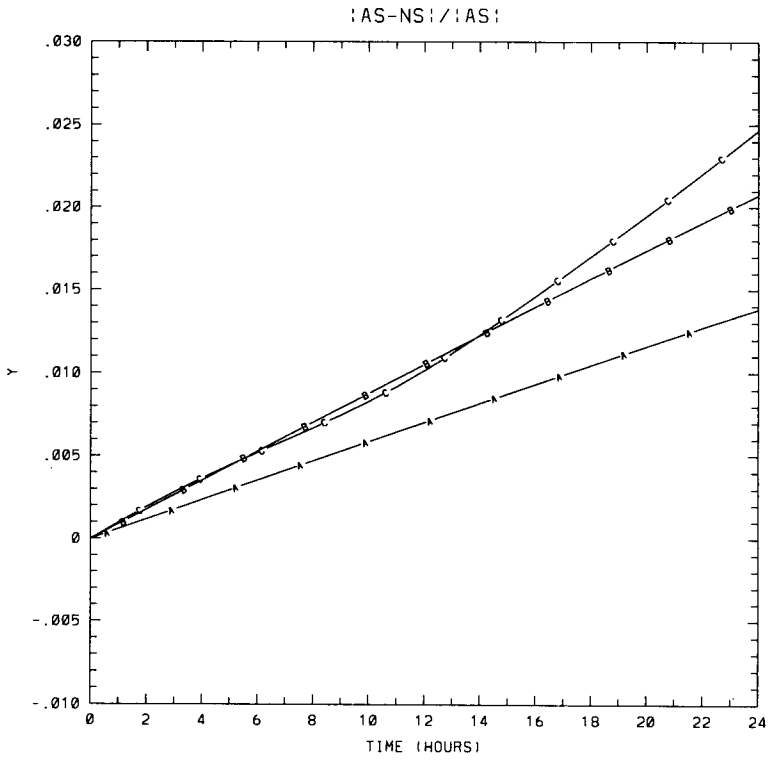

Fig. 6. The behavior of relative error (24) for the Rossby-Haurwitz wave (A), Wu-Verkley solution (B) and small Verkley's modon (C) during first 24 hours.

5) *Interaction of two modons.* Suppose that at the initial moment $t = 0$, a BVE solution ψ is the sum of two Verkley's modons Φ and Ψ whose centers are at the same latitudinal circle: $\psi(0) = \Phi(0) + \Psi(0)$. Then at a moment t, solution $\psi(t)$ can be written as

$$\psi(t) = \Phi(t) + \psi'(t) \tag{39}$$

where $\psi'(t)$ is considered as a perturbation of the modon $\Phi(t)$. Obviously, $\psi'(0) = \Psi(0)$, that is the initial perturbation has the form of the modon Ψ. The perturbation $\psi'(t)$ is governed by a forced equation

$$\Delta\psi'_t + J(\psi',\ \Delta\psi' + 2\mu) = F(\psi') \equiv J(\Delta\psi',\ \Phi) + J(\Delta\Phi, \psi') \tag{40}$$

If the modons Φ and Ψ initially are widely spaced then forcing $F(\psi')$ is relatively small, and the behavior of perturbation $\psi'(t)$ at the initial stage is similar in appearance to that of the modon $\Psi(t)$. In particular, if modons $\Psi(t)$ and $\Phi(t)$ initially differ from each other only in their locations ($\Psi(0,\ \lambda,\ \mu) = \Phi(0,\ \lambda+\lambda_o,\ \mu)$) then $F(\psi') = 0$, and $\psi'(t) = \Psi(t)$ for all t. It is a trivial case when the sum of two solutions of the nonlinear equation (1) is also an exact solution. This situation was numerically simulated with the T31-model when there are two equal modons of intermediate size ($k = 2,\ \alpha = 4,\ \mu_o = 0,\ \mu_a = \sin 36.5^o$, and $D_o = 0$) that move rather rapidly. The streamfunction of such solution is presented in Figures 7a-d at $t = 0$, and after 24, 48 and 72 hours of the integration.

We now consider the general case of two modons Φ and Ψ of different size and velocity. As Φ and Ψ we take the rapidly moving large-size modon given in Figure 4c and not so rapid medium-size modon given in Figure 7a. The integration was performed with the T31-model and very small time step $\Delta t = 20''$. As long as two modons are separated, the behavior of perturbation $\psi'(t)$ again resembles that of the modon Ψ. However after some time, due to distinct velocities, the modons approach closely enough for nonlinear interaction to be sufficiently strong (Fig. 8a). During the nonlinear interaction, the evolution of perturbation $\psi'(t)$ is basically determined by the nonlinear resonance excited in nonlinear equation (40) by the forcing $F(\psi')$. It is seen that both the amplitude and size of the medium-size modon increase at the expense of the energy loss and amplitude decrease in the large-size modon (Fig. 8b-e). The result of the nonlinear interaction is determined by the geometric structure of the forcing and appears as if two modons has changed their places. Evidently, this transformation can not be explained by the advective process, since both the modons move to the east, and after the interaction (Fig. 8e), the smaller modon is behind its initial position given in Figure 8a. We can see that when the system recovers from the resonance, the large-size modon survives after interaction, while the medium-size modon disappears (Fig. 8f). This fact counts in favour of the structural stability of the large-size modon to small-scale perturbations.

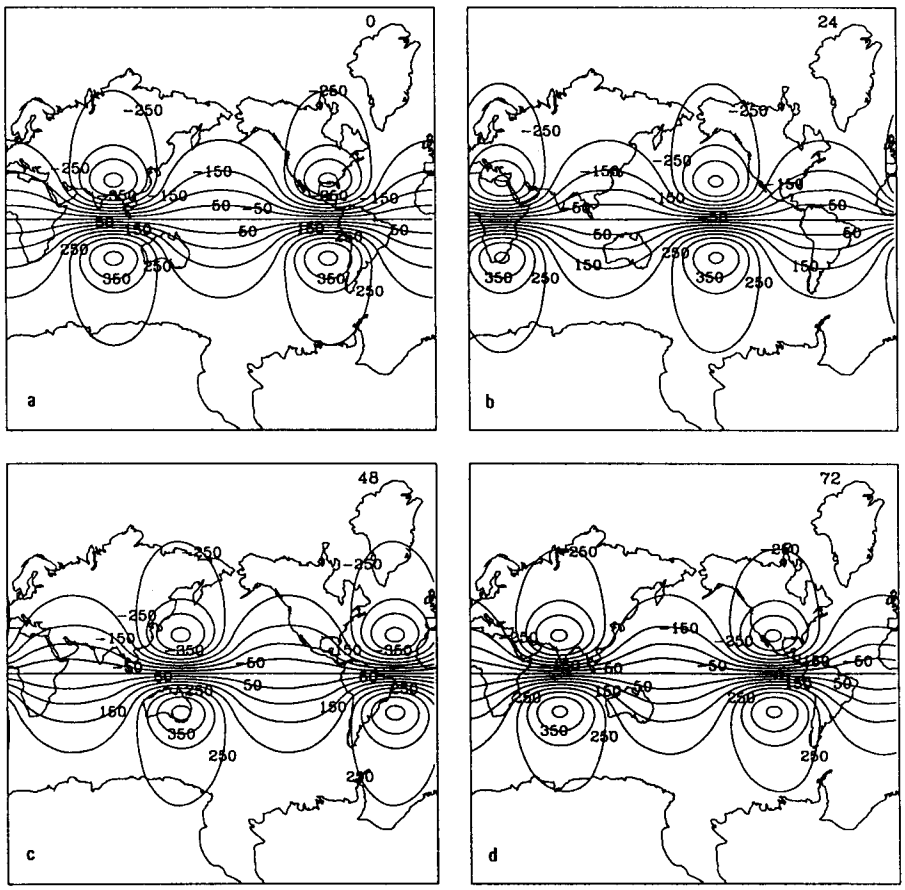

Fig. 7. The streamfunction of the BVE solution that initially is the sum of two equal medium-size modons separated from each other: $t = 0$ (a), $t = 24$ hours (b), $t = 48$ hours (c), and $t = 72$ hours (d). The contour interval is 50 m^2/s.

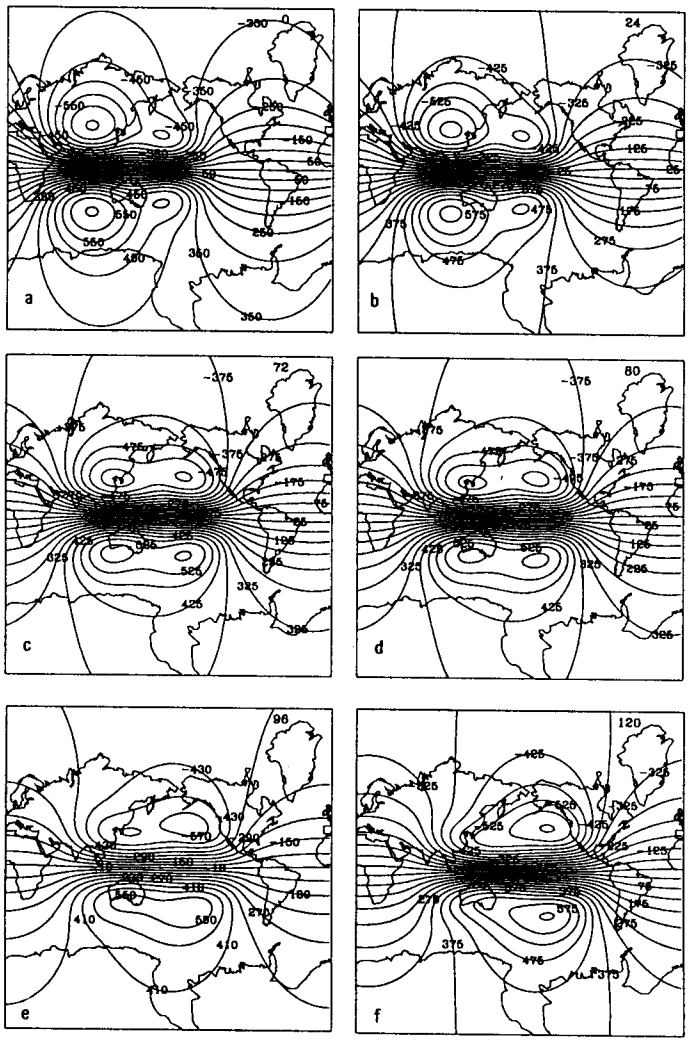

Fig. 8. Nonlinear interaction of two modons. The streamfunction of the BVE solution that initially is the sum of the medium-size modon given in Figure 7 and large-size modon given in Figure 4c at $t = 0$ (a), $t = 24$ min (b), $t = 72$ min (c), $t = 80$ min (d), $t = 96$ min (e), and $t = 120$ min (f).

4. Concluding remarks

Well-known exact solutions of the barotropic vorticity equation on a rotating sphere have been simulated with the numerical spectral model of the Center for Atmospheric Sciences, UNAM. Primary emphasis is received to preserving both the principal integral invariants of motion (kinetic energy and enstrophy) and the geometric structure of analytical BVE solutions on a sphere (zonal flows, Rossby-Haurwitz waves, Wu-Verkley solutions, and Verkley's dipole modons). As the quantitative characteristics of the proximity of the numerical and analytical solutions we have used the absolute and relative errors (24) estimated with $L_2(S)$-norm.

The 10-day integrations carried out with the triangularly truncated (T20, T31) models show that the classical exact solutions (RH waves) can be calculated to a good approximation. Besides, the larger is the spatial scale of the wave, the higher is the accuracy. However, the relative errors (24) obtained in calculating the generalized solutions (Wu-Verkley waves, modons) are larger as

compared with the classical solutions. These errors are caused not only by the truncation of Fourier's series that breaks the balanced energy cascade of the original differential model and leads to the energy dispersion, but also by the initial and structural instability of the solutions. In particular, the instability of some exact generalized solutions, notably rapidly moving dipole modons, with respect to initial and forcing errors is a serious obstacle in simulating long-time behavior of such solutions. If it is the case then even highly truncated model fails to resolve the problem, and the paths of the numerical and exact solutions diverge from each other with time. Nevertheless, the total energy and integral enstrophy of all the numerical solutions are conserved with a high degree of precision.

Acknowledgements

This work was supported by the DGSCA/UNAM-CRAY Research Inc. projects SC-006196 and SC-008097 and PAPIIT grant IN122098. We are thankful to Mr. A. Aguilar for programming assistance in preparation of the figures, to Mrs. María E. Castillo for typing the first draft of the manuscript, to Mrs. Thelma del Cid for editing the text, and Mrs. M. E. Grijalva for the final preparation of the paper. The comments and suggestions from the anonymous reviewers are gratefully appreciated.

REFERENCES

Adem J., 1956. A series solution for the barotropic vorticity equation and its application in the study of atmospheric vortices. *Tellus*, **8** (3), 364-372.

Andrews, D. G., 1984. On the stability of forced non-zonal flows. *Quart. J. R. Met. Soc.*, **110**, 657-662.

Baer, F., and G. W. Platzman, 1961. A procedure for numerical integration of the spectral vorticity equation. *J. Meteorology*, **18** (3), 393-401.

Baer, F., 1964. Integration with the spectral vorticity equation. *J. Atmos. Sci.*, **21**, 260-286.

Berestov, A. L., 1979. Solitary Rossby waves. *Izvestiya, Atmos. Ocean. Physics*, **15** (6), 648-654 (in Russian).

Blender, R., 1992. Approximate calculation of solitons and modons. *Beitr. Phys. Atmosph.*, **65** (4), 251-257.

Blinova, E. N., 1946. On the determination of the velocity of cyclones from nonlinear vorticity equation. *Appl. Math. Mechanics*, **10**, 5-6 (in Russian).

Blinova, E. N., 1956. Method of solving a nonlinear problem on atmospheric movements on a planetary scale. *Doklady Akad. Nauk SSSR*, **110** (5).

Boer, G. J., 1983. Homogeneous and isotropic turbulence on the sphere. *J. Atmos. Sci.*, **40** (1), 154-163.

Branstator, G., 1985. Analysis of general circulation model sea-surface temperature anomaly simulations using a linear model. Part II. Eigenanalysis. *J. Atmos. Sci.*, **42**, 2242-2254.

Bulgakov, S. N., 1996. *Black Sea Large-Scale Circulation and Water Stratification Formation. Buoyancy Flux Impact.* NAS of Ukraine, Sevastopol, Ukraine, ECOSI-Hydrophysica Pub., 243 pp. (in Russian).

Craig, R. A., 1945. A solution of the nonlinear vorticity equation for atmospheric motion. *J. Meteorology*, **2**, 173-178.

Dikii, L. A., 1976. *Hydrodynamic Stability and Atmosphere Dynamics.* Gidrometeoizdat, Leningrad, Russia (in Russian).

Ellsaesser, H. W., 1966. Evaluation of spectral versus grid methods of hemispheric numerical weather prediction. *J. Appl. Meteorology*, **5** (3), 246-262.

Ertel, H., 1943.Über statinäre oszillatorische luftströmungen auf der rotierenden erde. *Meteor. Zeits*, **60**, 332-334.

Fjörtoft, R., 1953. On the changes in the spectral distribution of kinetic energy for two-dimensional nondivergent flow. *Tellus*, **5** (3), 225-230.

Gary, J., 1979. Nonlinear instability. In: *Numerical Methods Used in Atmospheric Models*, Chapter 10, GARP Publication Series, WMO, No. 17, Vol.2.

Gill, A. E., 1982. *Atmosphere-Ocean Dynamics.* Academic Press, New York.

Golub, G. H., and J. M. Ortega, 1992. *Scientific Computing and Differential Equations. An Introduction to Numerical Methods.* Academic Press, Boston.

Haurwitz, B., 1940. The motion of atmospheric disturbances on the spherical earth. *J. Marine Research*, **3**, 254-267.

Helgason, S., 1984. *Groups and Geometric Analysis, Integral Geometry, Invariant Differential Operators and Spherical Functions.* Academic Press, Orlando.

Hoskins, B. J., 1973. Stability of the Rossby-Haurwitz wave. Quart. *J. R. Met. Soc.*, **99**, 723-745.

Kanehisa, H., 1994. An exact modon solution in a parabolically sheared zonal flow. *J. Meteorol. Soc. Japan*, **72** (5), 773-776.

Larichev, V. D., and G. M. Reznik, 1976. Two-dimensional Rossby soliton: An exact solution. Doklady Akad. Nauk SSSR, **231** (5), 1077-1079.

Legras, B., and M. Ghil, 1985. Persistent anomalies, blocking and variations in atmosphere predictability. *J. Atmos. Sci.*, **42**, 433-471.

Longuet-Higgins, M. S., and A. E. Gill, 1967. Resonant interactions between planetary waves. *Proc. R. Soc.*, **A 299**, 120-140.

Machenhauer, B., 1979. Spectral methods. In: *Numerical Methods Used in Atmospheric Models*, Chapter 3, GARP Publication Series, WMO, No. 17, Vol.2, 124-275.

McWilliams, J. C., G. R. Flierl, V. D. Larichev, and G. M. Reznik, 1981. Numerical studies of barotropic modons. *Dyn. Atmos. Oceans*, **5**, 219-238.

McWilliams, J. C., and N. J. Zabusky, 1982. Interactions of isolated vortices. *Geophys. Astrophys. Fluid Dynamics*, **19**, 207-227.

Merilees, Ph. E., 1968. The equations of motion in spectral form. *J. Atmos. Sci.*, **25**, 736-743.

Merilees, Ph. E., and H. Warn, 1975. On energy and enstrophy exchanges in two-dimensional non-divergent flow. *J. Fluid Mechanics*, **69**, 625-630.

Mesinger, F., and A. Arakava, 1976. *Numerical Methods Used in Atmospheric Models*, GARP Publication Series, WMO, No. 17, Vol.1.

Morton, K. W. and D. F. Mayers, 1994. *Numerical Solution of Partial Differential Equations.* Cambridge University Press, Cambridge.

Neamtan, S. M., 1946. The motion of harmonic waves in the atmosphere. *J. Meteorology*, **3**, 53-56.

Neven, E. C., 1992. Quadrupole modons on a sphere. *Geophys. Astrophys. Fluid Dynamics,* **65**, 105-126.

Neven, E. C., 1993. *Modons on a Sphere.* Universiteit Utrecht, Utrecht, Nederlands, 175 pp.

Piterbarg, L. I., 1998. Hamiltonian formalism for Rossby waves. *Amer. Math. Soc. Transl. Series,* **182** (2), 131-166.

Platzman, G. W., 1960. The spectral form of the vorticity equation.*J. Meteorology,* **17**, 635-644.

Platzman, G. W., 1962. The analytical dynamics of the spectral vorticity equation. *J. Atmos. Sci.,* **19**, 313-328.

Richtmyer, R. D., 1981.*Principles of Advanced Mathematical Physics.* Springer-Verlag, Vol. 2.

Rochas, M., 1986. A new class of exact time-dependent solutions of the vorticity equation. *Mon. Wea. Rev.,* **114**, 961-966.

Rossby, C.-G., 1939. Relation between variations in the intensity of the zonal circulation of the atmosphere and the displacements of the semipermanent centers of action. *J. Mar. Res.,* **2**, 38-55.

Silberman, I., 1954. Planetary waves in the atmosphere. *J. Meteorology,* **11** (1), 27-34.

Skiba, Yu. N., 1989. *Mathematical Problems of the Dynamics of Viscous Barotropic Fluid on a Rotating Sphere.* Dept. Comput. Mathematics, The USSR Academy of Sciences, Moscow, 178 pp. (English transl.: Indian Institute of Tropical Meteorology, Pune, India, 1990, 211 pp.).

Skiba, Yu. N., 1991. Lyapunov instability of the Rossby-Haurwitz waves and dipole modons. *Sov. J. Numer. Analysis & Mathem. Modelling,* **6**, 515-534.

Skiba, Yu. N., 1992a. On stability of Rossby-Haurwitz waves. *Izvestiya, Atmos. Ocean. Physics,* **28** (5), 388-394.

Skiba, Yu. N., 1992b. On Stability of barotropic modons on a sphere. *Izvestiya, Atmos. Ocean. Physics,* **28** (10-11), 765-773.

Skiba, Yu. N., 1993. Dynamics of perturbations of the Rossby-Haurwitz wave and the Verkley modon. *Atmósfera,* **6**, 87-125.

Skiba, Yu. N., 1994. On the long-time behavior of solutions to the barotropic atmosphere model. *Geophys. Astrophys. Fluid Dynamics,* **78**, 143-167.

Skiba, Yu. N., 1996. On asymptotic regimes of the barotropic vorticity equation on a sphere. *Russian Meteorology and Hydrology,* **3**, 37-45.

Skiba, Yu. N., 1997. On dimensions of attractive sets of viscous fluids on a sphere under quasi-periodic forcing. *Geophys. Astrophys. Fluid Dynamics,* **85** (3-4), 233-242.

Skiba, Yu. N., 1998. Spectral approximation in the numerical stability study of non-divergent viscous flows on a sphere. *Numerical Methods for Partial Differential Equations,* **14**, 143-157.

Skiba, Yu. N., and J. Adem, 1998. On the linear stability study of zonal incompressible flows on a sphere. *Numerical Methods for Partial Differential Equations,* **14**, 649-665.

Stern, M. E., 1975. Minimal properties of planetary eddies. *J. Mar. Res.,* **33**, 1-13.

Szeptycki, P., 1973. Equations of hydrodynamics on manifold diffeomorfic to the sphere. *Bull. L'acad. Pol. Sci., Ser. Sci. Math. Astr. Phys.,* **21** (4), 341-344.

Temam, R., 1998. *Infinite-Dimensional Dynamical Systems in Mechanics and Physics,* Springer, NY.

Thompson, P. D., 1982. A generalized class of exact time-dependent solutions of the vorticity equation for nondivergent barotropic flow. *Mon. Wea. Rev.,* **110**, 1321-1324.

Topuriya, S. B., 1987. *Fourier-Laplace Series on a Sphere.* Tbilisi University Press, Tbilisi, USSR (in Russian).

Tribbia, J. J., 1984. Modons in spherical geometry, Geophys. *Astrophys. Fluid Dynamics,* **30**, 131-168.

Verkley, W. T. M., 1984. The construction of barotropic modons on a sphere. *J. Atmos. Sci.,* **41** (16), 2492-2504.

Verkley, W. T. M., 1987. Stationary barotropic modons in westerly background flows. *J. Atmos. Sci.,* **44**, 2383-2398.

Verkley, W. T. M., 1989. *On Atmospheric Blocking and the Theory of Modons.* K.N.M.I., Vrije Universiteit te Amsterdam, Utrecht, Nederlands, 171 pp.

Verkley, W. T. M., 1990. Modons with uniform absolute vorticity. *J. Atmos. Sci.,* **47**, 727-745.

Wiin-Nielsen, A., 1979. Steady states and stability properties of a long-order barotropic system with forcing and dissipation. *Tellus,* **31**, 375-386.

Wu, P., and W. T. M. Verkley, 1993. Non-linear structures with multivalued (q, ψ) relationships - exact solutions of the barotropic vorticity equation on a sphere. *Geophys. Astrophys. Fluid Dynamics,* **69**, 77-94.

Wu, P., 1993. Nonlinear resonance and instability of planetary waves and low-frequency variability in the atmosphere. *J. Atmos. Sci.,* **50** (21), 3590-3607.

Zalesny, V. B., 1986. Numerical model of ocean dynamics based on the splitting-up method. *Sov. J. Numerical anal. Math Modelling.* **1**, 141-162.